Progress In Electromagnetics Research, Vol. 107, 413–425, 2010

A COMPACT PLANAR HEXA-BAND INTERNAL ANTENNA FOR MOBILE PHONE

J.-Y. Sze and Y.-F. Wu

Department of Electrical and Electronic Engineering
Chung Cheng Institute of Technology
National Defense University
190 Sanyuan 1st. St., Dasi Township
Taoyuan County 33508, Taiwan, R.O.C.

Abstract—A planar hexa-band internal antenna designed for mobile phone applications is presented. The antenna occupying a small area of $45 \times 12\,\text{mm}^2$ is placed on the top no-ground portion of the system circuit board with a ground-plane size of $45 \times 100\,\text{mm}^2$. The design begins with constructing a meandered monopole. With a parasitic and an impedance-adjustment structure subsequently added, the resulting antenna can be viewed as a printed planar inverted-F antenna with a parasitic resonant element. Two wide impedance bands can be generated by the designed antenna to support GSM 850, GSM 900, DCS, PCS, UMTS, and 2.4-GHz WLAN operations. The measurement was found to agree reasonably well with the simulation. Design procedures and rules along with the design concepts behind are all presented in detail.

1. INTRODUCTION

In recent years, handheld mobile wireless communication devices (especially mobile phones) have been widely and rapidly developed. External appearances of these devices have been receiving increasingly more attention. Besides keeping the appearances attractive, these devices must be small not only in the plane parallel to the screen but also in the thickness direction for becoming competitive in the market. For attractiveness in appearance, internal antennas that can be completely concealed in the case of a mobile phone are now prevailing over external antennas [1–20]. However, the trend

Received 6 February 2010, Accepted 12 August 2010, Scheduled 27 August 2010
Corresponding author: J.-Y. Sze (jeffszejy@gmail.com).

for an upcoming mobile phone is that more components need to be installed inside to make the mobile phone more powerful yet possibly smaller in overall size. Hence, quite unfortunately, the space in a mobile phone that can be allocated to deploy an internal antenna becomes more and more limited. In addition, for better functionality, most internal mobile-phone antennas are required to provide operating bands wide enough to support the following five communication standards: GSM 850 (824–894 MHz), GSM 900 (880–960 MHz), DCS (1710–1880 MHz), PCS (1850–1990 MHz), and UMTS (1920–2170 MHz). Communication networks involving these standards are usually referred to as wireless wide-area networks (WWANs). In order to access the internet, an additional band of 2.4–2.484 GHz for WLAN applications is also desirable for the antenna mounted internal to a mobile handset.

For ease of fabricating mobile handsets, printed internal antennas have been designed to be integrated with ground planes and system circuits on the same substrates [5–20]. Since the substrates employed are usually very thin and the conductors printed on them are even much thinner, it is safe to describe antennas of these types only by their widths and heights, without emphasizing their thicknesses. These antennas can be divided into four groups. Loop antennas in the first group are operated as a half-wavelength resonant structure [5, 6]. Although being able to achieve penta-band operations for GSM 850, GSM 900, DCS, PCS, and UMTS, antennas in this group suffer from the drawback of having a large radiator area (as large as 900 mm^2). In the second group, monopole antennas are operated as a quarter-wavelength resonant structure [7–11]. When the radiator in this type of antenna is close to the ground plane, the resulting intensive coupling effect between the radiator and the ground plane usually makes it difficult to design a quarter-wavelength monopole antenna that not only preserves a small antenna height and width but also achieves the desired hexa-band operations. In this group, the antenna in [7] ([9]) although having a small antenna area of $38.5 \times 15 = 577.5\,mm^2$ ($60 \times 10 = 600\,mm^2$) can support only the following five communication standards: GSM 900, DCS, PCS, UMTS, and 2.4-GHz WLAN (GSM 850, GSM 900, DCS, PCS, and UMTS). Belonging to the third group, monopole slot antennas can also be operated as a quarter-wavelength resonant structure if the slot is cut at the edge of the ground plane [12–15]. The monopole slot antenna designed in [15] has a small size of $40 \times 15 = 600\,mm^2$ and can support the desired hexa-band operations. However, a height of 15 mm may be regarded as too large for some mobile handsets. In the fourth group are printed planar inverted-F antennas (printed

PIFAs) [16–20], whose operations also rely on quarter-wavelength resonance. A simple printed PIFA can be constructed by adding a grounded strip to an inverted-L quarter-wavelength monopole [16, 17]. The height of a simple printed PIFA is usually smaller than those of other types of antennas. However, a smaller height implies a more intensive coupling effect between the radiator and the ground plane, leading to a larger capacitive reactance and hence a poorer impedance match. Although the impedance mismatch owing to the intensive coupling effect can be improved by adding a grounded strip that acts as an impedance-adjustment structure, the resulting impedance bandwidth is often still not large enough. This is why simple printed PIFAs [16, 17] are frequently adopted in the 2.4- and 5.2-GHz WLAN bands, for which the required fractional bandwidths are only moderate, but not in other lower frequency bands for which the required fractional bandwidths are relatively large. To overcome this disadvantage, some research papers [18–20] have proposed printed PIFAs using coupling feeding structures, instead of the direct feeding ones employed in [16, 17]. These antenna designs not only can support WWAN or WWAN/WLAN operations but also have smaller antenna heights (i.e., 11, 11, 10 mm for the antennas in [18–20], respectively) than those in most of the antennas in [5–15]. Among them, the antenna in [20], although having the smallest antenna height of 10 mm, can support GSM 850/900/DCS/PCS/UMTS/2.4-GHz WLAN hexa-band operations. However, the antenna width of 60 mm for the antennas in [16, 18] may be considered large for some handsets.

In this paper, we aim to design for the desired hexa-band (WWAN and WLAN) operations an internal printed direct-fed antenna that has an width of 45 mm and that has an area of only $45 \times 12 = 540\,\text{mm}^2$, which is smaller than those of all the mobile-phone antennas in [5–15, 20] (note that the antennas in [16, 17] are for WLAN operations only and those in [18, 19] are for laptop-computer applications). In particular, the width (height) of 45 mm (12 mm) is smaller than those of the antennas in [5, 9, 18–20] ([5–8] and [13–15]). The designed antenna is expected to provide two impedance bands, the lower (upper) of which should cover the desired operating band of 824–960 MHz (1710–2484 MHz) required by GSM 850 and GSM 900 (DCS, PCS, UMS, and 2.4-GHz WLAN). Although the designed antenna can be viewed as a printed PIFA with a parasitic grounded inverted-L strip nearby, it was actually constructed to be only a meandered monopole in the initial design stage. With the excitation mechanism and impedance matching of various resonant modes of the printed monopole presented step by step, systematic design procedures and rules are developed to achieve the goal.

2. ANTENNA CONFIGURATION

Figure 1 shows the geometry of the proposed planar internal antenna, which is fabricated using a 0.8-mm-thick, 45-mm-wide, and 112-mm-high FR4 substrate with dielectric constant 4.4. On the lower portion of the FR4 substrate is a $45 \times 100\,\text{mm}^2$ ground plane, above which is an area of $45 \times 12\,\text{mm}^2$ (referred to as the antenna area for convenience) reserved to locate the designed antenna. The designed antenna, according to its inherent functions, can be divided into three parts: a main radiation structure (or called a main radiator), a parasitic structure, and an impedance-adjustment structure (see the detailed metal pattern in Fig. 1(b)); all these structures are printed coplanar with the ground plane. The main radiator is a 1-mm-wide, 80-mm-long metal strip that starts from the upper-right corner and is printed along the E-D-C-B-A meandered path. This strip, which is to be excited at point A and whose bottom edge is 1-mm away from the ground plane, can be designed to resonate at about 960 and 2100 MHz. The parasitic structure lies in the lower-right corner of the antenna area and is a 1-mm-wide grounded inverted-L metal strip. This strip originates from

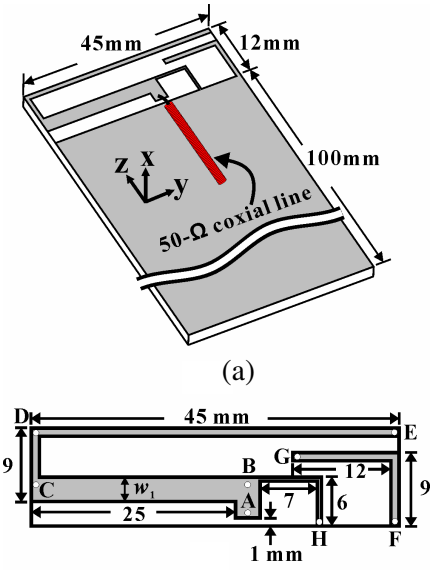

Figure 1. Compact planar hexa-band antenna for a mobile phone: (a) perspective view of the entire structure, (b) metal pattern in the antenna area.

point F of the ground plane, extends upward along the right edge of the substrate by a length of 9 mm, and then extends leftward by a length of 12 mm. The parasitic structure is implemented to excite one additional resonant mode to widen the upper impedance band. The impedance-adjustment structure is a 0.5-mm-wide inverted-L strip, whose 7-mm-long horizontal section connects to point B of the main radiator and whose 6-mm-long vertical section connects to point H of the ground plane. This structure can improve the impedance matching in the lower impedance band. Finally, the AB and BC sections of the main radiator are widened to have a width of 3 mm, resulting in a much better impedance match in the upper resonant band. The design procedures along with the design ideas behind are elucidated in the next section.

3. CONCEPTS AND PROCEDURES OF ANTENNA DESIGN

3.1. Preliminary Design of Main Radiator

For size reduction, many existing multi-band monopole antennas have been constructed by bending a metal strip into meandered shape. The meandered strip can be designed to resonate around multiple pre-selected frequencies. The quarter-wavelengths of the first few resonant modes are roughly the total length of the meandered strip or the lengths of some particular sections bent in the meandered strip. In this study, the main strip, whose route is E-D-C-B-A (see Fig. 1(b)) with a total length of 80 mm, is also of meandered type. For convenience, the antenna so constructed is a folded monopole antenna referred to as the type 1 antenna. As shown in Fig. 2, the first three

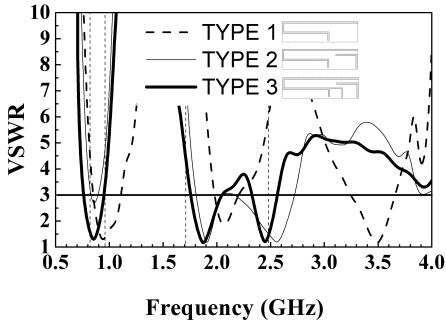

Figure 2. Measured VSWR against frequency for the types 1, 2, and 3 antennas.

resonant modes of the folded monopole antenna are excited at around 960, 2100, and 3500 MHz. Simulated using Ansoft HFSS, the electric current distributions of the resonant modes on the meandered strip of the type 1 antenna are shown in Fig. 3. The quarter-wavelength route of the electric current distribution at 960 MHz roughly has the same length of the entire main radiator, whereas the A-B-C quarter-wavelength route at 2100 MHz has a much shorter length of about 35.7 mm. For the third resonant mode at 3500 MHz, the half-wavelength route of the main electric current distributed between two current nulls (depicted as circular dashed lines in Fig. 3(c)) has a length of about 33 mm. Since the impedance band associated with the third resonant mode is far beyond our frequency bands of interest, the frequency response of that band will not be studied in the remaining antenna design procedures.

3.2. Design of Parasitic Structure

Note that the upper (i.e., the second) VSWR ≤ 3 impedance band of the type 1 antenna is far from wide enough to cover the desired higher operating band (i.e., 1710–2484 MHz) for DCS, PCS, UMTS, and 2.4-GHz WLAN operations. To achieve the goal, an additional

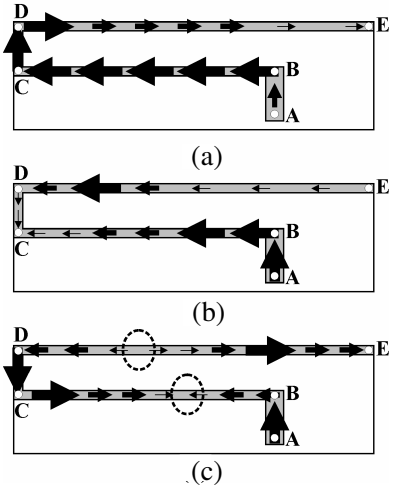

Figure 3. Resonant-mode electric current distributions on the type 1 antenna at (a) 960 MHz, and (b) 2100 MHz, (c) 3500 MHz.

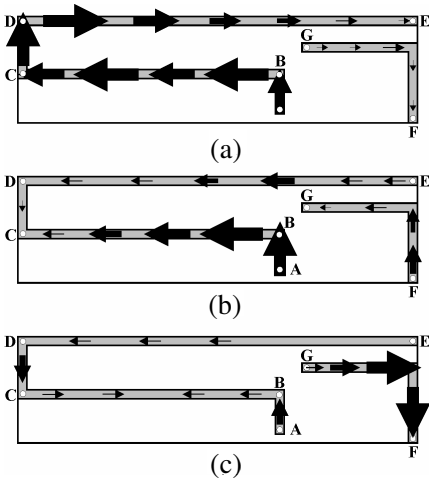

Figure 4. Resonant-mode electric current distributions on the type 2 antenna at (a) 850 MHz, and (b) 1907 MHz, (c) 2560 MHz.

resonant mode excited in the desired upper operating band is needed. For that purpose, a grounded inverted-L strip functioning as a parasitic structure is added in the lower-right corner of the antenna area to form a type 2 antenna. Note that the right edge of the vertical section of the parasitic structure is aligned with that of the substrate; the horizontal section of the parasitic structure is set to be equal vertical distance away from the two horizontal sections (i.e., the DE and BC sections) of the main radiator.

With the length of the parasitic structure's vertical section fixed at 9 mm, the resonant mode excited in the parasitic structure can be controlled by varying the length of the horizontal section. When the length of the horizontal section is adjusted to 12 mm, the additional resonant mode is excited at about 2500 MHz, whereas the first and second resonant frequencies are slightly lowered from 960 and 2100 MHz of the type 1 antenna to 850 and 1907 MHz, respectively. The changes in resonant frequencies can be explained by examining on the type 2 antenna the electric current distributions depicted in Fig. 4. Because of the presence of the parasitic structure, the open end of the meandered strip around point E experiences a larger fringing capacitance, resulting in a larger effective length of the meandered strip than that of the type 1 antenna. Hence, although the current distributions of the first two resonant modes on the meandered strips of the types 1 and 2 antennas are very similar, the resonant frequencies of the latter are slightly lower than those of the former. By contrast, the quarter-wavelength current distribution of the additional (third) resonant mode shown in Fig. 4(c) mainly concentrates on the parasitic structure of the type 2 antenna, and the associated current distribution on the meandered strip is much weaker and is quite different from that of the third resonant mode of the type 1 antenna. The resonance occurring mainly in the parasitic structure instead of the main radiator explains why the third resonant frequency of the type 2 antenna is farther away from that of the type 1 antenna than are the first two resonant frequencies of the type 2 antenna away from those of the type 1 antenna. Since the two resonant frequencies of the second and third excited modes are close to each other, a wide upper impedance band of 1800–2720 MHz is established. Unfortunately, the parasitic structure has downgraded the impedance matching in the lower resonant band, leading to a minimum VSWR of as high as 2.7 in that band.

3.3. Design of Impedance-adjustment Structure

For the type 2 antenna, the enhancement in the upper impedance bandwidth accompanies an impedance mismatch in the lower resonant

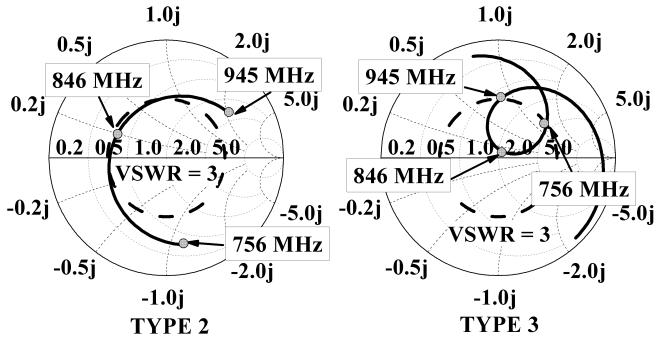

Figure 5. Reflection-coefficient loci around the lower resonant bands for the types 2 and 3 antennas.

band. To overcome this problem, we sought to adjust the input impedance, especially in the lower resonant band. With a 0.5-mm-wide grounded inverted-L strip connected to point B of the main radiator to form a type 3 antenna, the first three resonant modes are excited around the frequencies that are close to the resonant frequencies of the type 2 antenna (the current distributions on the meandered strips of these two antennas are very similar and are not shown here for brevity). This grounded inverted-L strip provides adequate impedance matching in the lower resonant band (see Fig. 2) and hence can be used as the impedance-adjustment structure. The reflection-coefficient loci of the types 2 and 3 antennas are shown in the Smith charts of Fig. 5. This impedance-adjustment structure helps improve the impedance matching in the lower resonant band around 850 MHz, leading to a tightened resonant locus in the Smith chart for the type 3 antenna. The resulting lowest VSWR is as low as 1.2, and the VSWR ≤ 3 impedance band now ranges from 756 to 945 MHz, only slightly insufficient to cover the desired lower operating band (i.e., 824–960 MHz) for GMS 850 and GMS 900 operations.

3.4. Final Design of Main Radiator for Better Impedance Matching

Although the impedance matching in the lower resonant band of the type 3 antenna is greatly improved as compared with the type 2 antenna, the impedance matching around 2.2 GHz in the upper impedance band is downgraded. Obviously, the type 2 antenna's upper VSWR ≤ 3 impedance band has been split into the type 3 antenna's two disjoint bands, which are even more insufficient for completely

enclosing the desired upper operating band of 1710–2484 MHz. To overcome this problem, the strong variation of the electric current on the main radiator needs to be smoothened. This can be accomplished by widening the A-B-C section of the main radiator. The horizontal BC section is widened toward the $-z$ direction, whereas the vertical AB section is widened symmetrically toward the $+y$ and $-y$ directions. With the width (w_1) of the A-B-C section changed from 1 to 3 mm, not only can the upper VSWR ≤ 3 impedance band be enlarged to 1705–2505 MHz, but a lower impedance band of 810–1010 MHz can also be obtained, as shown in Fig. 6. Each of these two impedance bands can completely cover its associated desired operating band. Hence, the type 3 antenna with $w_1 = 3$ mm is selected to be our final designed antenna. From Fig. 7, it is observed that the electric current on BC section is smoothened after widening the width of the A-B-C section.

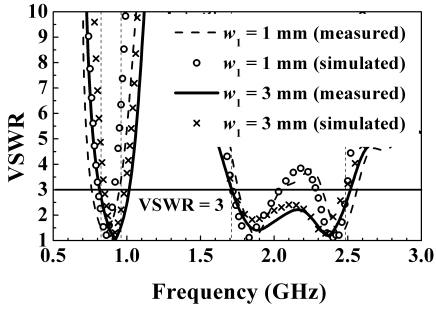

Figure 6. Measured VSWR for the type 3 antenna with different vales of w_1.

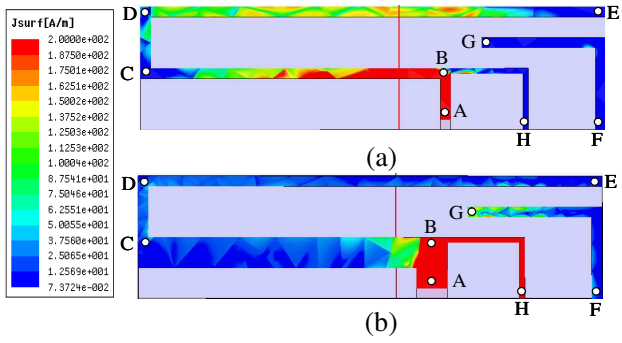

Figure 7. Simulated electric current distributions of type 3 antenna at 2200 MHz with different vales of w_1: (a) $w_1 = 1$ mm; (b) $w_1 = 3$ mm.

3.5. Radiation Characteristics of the Designed Antenna

Figure 8 shows for the final designed antenna the measured and simulated far-field radiation patterns in the x-y, y-z, and x-z planes

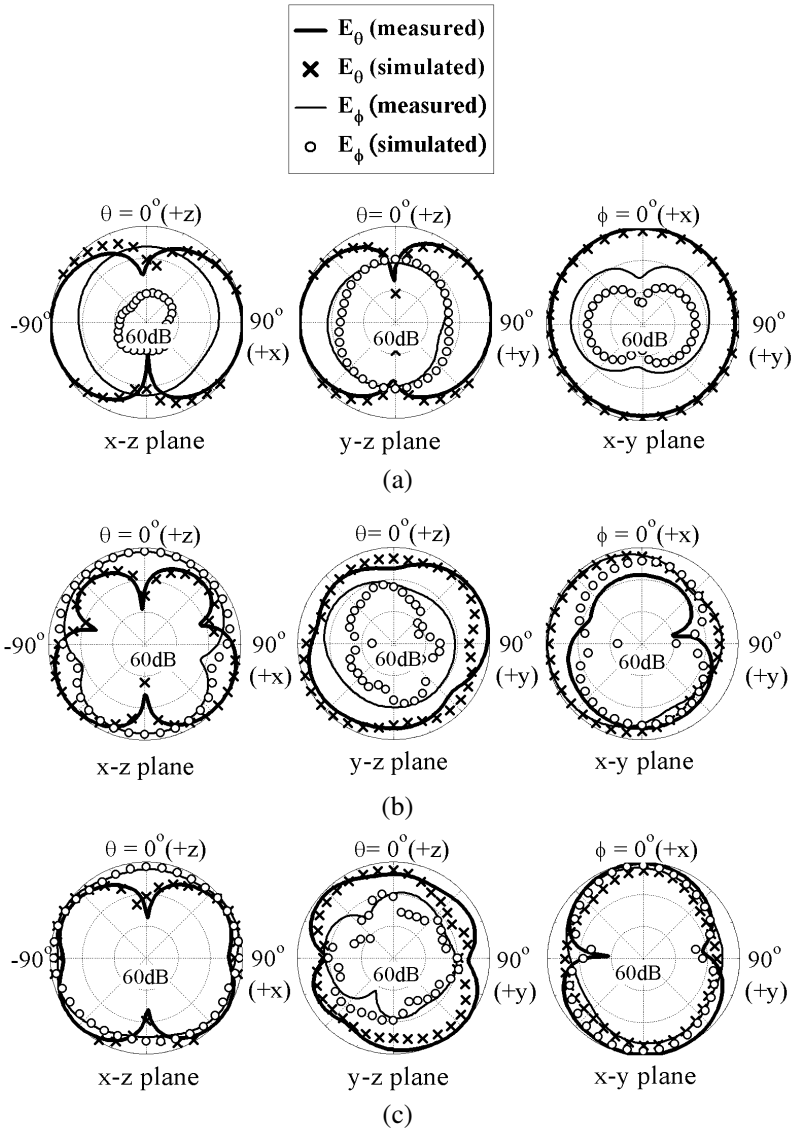

Figure 8. Measured and simulated far-field radiation patterns for the three resonant modes of the designed antenna at (a) 920 MHz, (b) 1880 MHz, and (c) 2365 MHz.

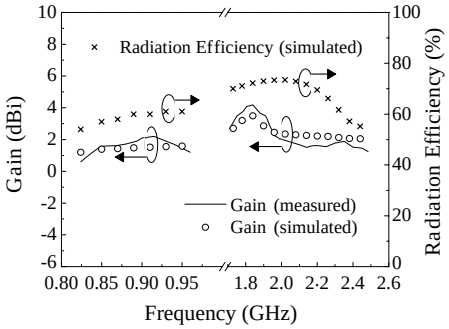

Figure 9. Peak antenna gains and antenna efficiencies in the two operating bands of the designed antenna.

at the frequencies of the three resonant modes. The measured and simulated results agree reasonably well with each other. Shown in Fig. 9 are the measured and simulated peak antenna gains and the simulated antenna efficiency. The peak antenna gain in the lower operating band is in the range of 0.6–2.2 dBi and that in the upper, 1.5–4.2 dBi; the efficiencies in the lower and upper operating bands are around 60% and 70%, respectively, rendering the designed antenna suitable for practical applications.

4. CONCLUSION

A planar hexa-band internal antenna proposed in this paper has been successfully realized and discussed. The antenna was initially designed as a meandered monopole and subsequently step-by-step developed into a direct-fed printed PIFA with a parasitic resonant unit. The structurally simple antenna not only occupies a small area of only $45 \times 12\,\text{mm}^2$ but also has two VSWR ≤ 3 impedance bands of 810–1010 MHz and 1705–2515 MHz, which can cover the desired operating bands required for GSM 850, GSM 900, DCS, PCS, UMTS, and 2.4-GHz WLAN operations. This antenna was measured to have good radiation characteristics. The peak antenna gains in the lower and upper operating bands are as high as 1.5 and 3 dBi, respectively, making the antenna valuable for practical applications.

ACKNOWLEDGMENT

The authors would like to thank the reviewers for their careful review and valuable suggestions. This work was supported by the National

Science Council of Taiwan, ROC, under Grand NSC 95-2623-7-014-013-D. The authors are also grateful to the National Center for High-Performance Computing, Taiwan, ROC, for computing time and facilities.

REFERENCES

1. Mazinani, S. M. and H. R. Hassani, "A wideband internal plate loaded planar monopole antenna for mobile handset," *Journal of Electromagnetic Waves and Applications*, Vol. 23, No. 10, 1273–1282, 2009.
2. Chiu, C. W., C. H. Chang, and Y. J. Chi, "Multiband folded loop antenna for smart phones," *Progress In Electromagnetics Research*, Vol. 102, 213–226, 2010.
3. Sun, J. S. and S. Y. Huang, "A small 3-D multi-band antenna of "F" shape for portable phones' applications," *Progress In Electromagnetics Research Letters*, Vol. 9, 183–192, 2009.
4. Saidatul, N. A., A. A. H. Azremi, R. B. Ahmad, P. J. Soh, and F. Malek, "Multiband fractal planar inverted F antenna (F-Pifa) for mobile phone application," *Progress In Electromagnetics Research B*, Vol. 14, 127–148, 2009.
5. Chi, Y. W. and K. L. Wong, "Internal compact dual-band printed loop antenna for mobile phone application," *IEEE Trans. Antennas Propag.*, Vol. 55, No. 5, 1457–1462, May 2007.
6. Li, W. Y. and K. L. Wong, "Internal printed loop-type mobile phone antenna for penta-band operation," *Microwave Opt. Technol. Lett.*, Vol. 49, No. 10, 2595–2599, Oct. 2007.
7. Jing, X., Z. Du, and K. Gong, "A compact multiband planar antenna for mobile handsets," *IEEE Antennas Wirel. Propag. Lett.*, Vol. 5, 343–345, 2006.
8. Sim, C. Y. D., "Mutiband planar antenna design for mobile handset," *Microwave Opt. Technol. Lett.*, Vol. 50, No. 6, 1543–1545, Jun. 2008.
9. Wong, K. L. and T. W. Kang, "GSM 850/900/1800/1900/UMTS printed monopole antenna for mobile phone application," *Microwave Opt. Technol. Lett.*, Vol. 50, No. 12, 3192–3198, Dec. 2008.
10. Lin, D. B., I. T. Tang, and Y. Y. Chang, "Flower-like CPW-fed monopole antenna for quad-band operation of mobile handsets," *Journal of Electromagnetic Waves and Applications*, Vol. 23, No. 17–18, 2271–2278, 2009.

11. Chen, W. S. and B. Y. Lee, "A meander Pda antenna for GSM/Dcs/PCS/UMTS/WLAN applications," *Progress In Electromagnetics Research Letters*, Vol. 14, 101–109, 2010.
12. Cheng, P. C., C. Y. D. Sim, and C. H. Lee, "Multi-band printed internal monopole antenna for mobile handset applications," *Journal of Electromagnetic Waves and Applications*, Vol. 23, No. 13, 1733–1744, 2009.
13. Wong, K. L., Y. W. Chi, and S. Y. Tu, "Internal multiband printed folded slot antenna for mobile phone application," *Microwave Opt. Technol. Lett.*, Vol. 49, No. 8, 1833–1837, Aug. 2007.
14. Wu, C. H. and K. L. Wong, "Hexa-band internal printed slot antenna for mobile phone application," *Microwave Opt. Technol. Lett.*, Vol. 50, No. 1, 35–38, Jan. 2008.
15. Lin, C. I. and K. L. Wong, "Printed monopole slot antenna for internal multiband mobile phone antenna," *IEEE Trans. Antennas Propag.*, Vol. 55, No. 12, 3690–3697, Dec. 2007.
16. Tan, Q. and D. Erricolo, "Comparison between printed folded monopole and inverted F antennas for wireless portable devices," *Antennas and Propagation International Symposium*, 4701–4704, Jun. 2007.
17. Angelopoulos, E. S., A. I. Kostaridis, and D. I. Kaklamani, "A novel dual-band F-inverted antenna printed on a PCMCIA card," *Microwave Opt. Technol. Lett.*, Vol. 42, No. 2, 153–156, Jul. 2004.
18. Wong, K. L. and S. J. Liao, "Uniplanar coupled-fed printed PIFA for WWAN operation in the laptop computer," *Microwave Opt. Technol. Lett.*, Vol. 51, No. 2, 549–554, Feb. 2009.
19. Lee, C. T. and K. L. Wong, "Study of a uniplanar printed internal WWAN laptop computer antenna including user's hand effects," *Microwave Opt. Technol. Lett.*, Vol. 51, No. 10, 2341–2346, Oct. 2009.
20. Lee, C. T. and K. L. Wong, "Uniplanar coupled-fed printed PIFA for WWAN/WLAN operation in the mobile phone," *Microwave Opt. Technol. Lett.*, Vol. 51, No. 5, 1250–1257, May 2009.